Optimization Models for Planning Shale Gas Well Refracture Treatments

Diego C. Cafaro[1], Markus G. Drouven[2*] and Ignacio E. Grossmann[2]*

[1] INTEC (UNL – CONICET), Güemes 3450, 3000 Santa Fe, ARGENTINA

[2] Department of Chemical Engineering, Carnegie Mellon University, Pittsburgh, PA 15213, U.S.A.

ABSTRACT. Refracturing is a promising option for addressing the characteristically steep decline curves of shale gas wells. In this work we propose two optimization models to address the refracturing planning problem. First, we present a continuous-time nonlinear programming (NLP) model based on a novel forecast function that predicts pre- and post-treatment productivity declines. Next, we propose a discrete-time, multi-period mixed-integer linear programming (MILP) model that explicitly accounts for the possibility of multiple refracture treatments over the lifespan of a well. In an attempt to reduce solution times to a minimum, we compare three alternative formulations against each other (big-M formulation, disjunctive formulation using Standard and Compact Hull-Reformulations) and find that the disjunctive models yield the best computational performance. Finally, we apply the proposed MILP model to two case studies to demonstrate how refracturing can increase the expected recovery of a well and improve its profitability by several hundred thousand USD.

---

[*] Both authors contributed equally to this work.

Correspondence concerning this article should be addressed to D.C. Cafaro at dcafaro@fiq.unl.edu.ar

1. INTRODUCTION

Shale gas wells are well-known for their characteristically steep decline curves, as seen in Fig. 1. In fact, some shale wells may produce more than half of their total estimated ultimate recovery (EUR) within the first year of operation. The initial production peak after well completions is caused by the sudden release of previously trapped hydrocarbons in the pores of the reservoir. The subsequent decline is ultimately driven by pressure depletion and the ultralow permeability of the shale play. Upstream operators oftentimes struggle with the production decline curves. For one, they are contractually obligated to providing steady gas deliveries to midstream distributors over time – which is difficult to accomplish given that shale well production rates decline by as much as 65-85% within the first year after turning wells in line. Moreover, as Cafaro and Grossmann[1] suggest and Drouven and Grossmann[2] confirm, operators need to maximize the utilization of production and gathering equipment – such as pipelines and compressors – in order to stay profitable. In reality, however, production and gathering equipment is usually sized based on the initially high production rates. This means that within a matter of months shale gas wells feed into oversized pipelines and compressor stations, and equipment utilization drops. Even worse, in order to satisfy contractual gas delivery agreements, operators see themselves forced to open up new wells continuously to honor their obligations, and hence the process is repeated over and over again.

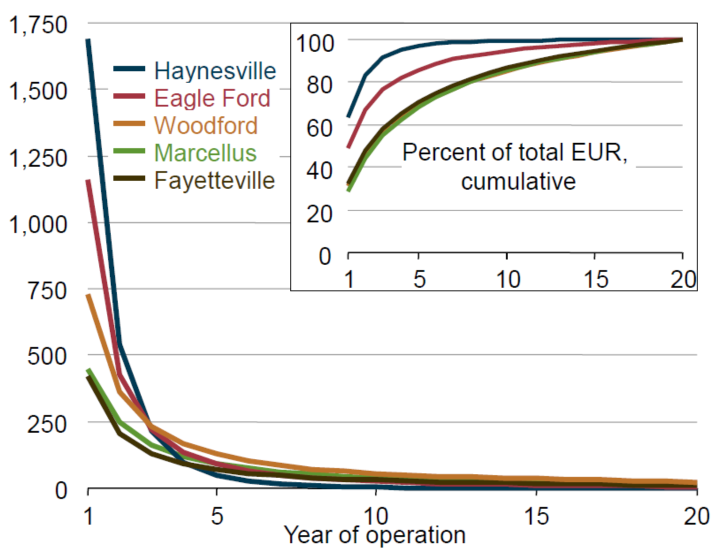

Fig. 1: Production profiles in million cubic feet per year for shale gas wells in major U.S. shale plays, Source: U.S. Energy Information Administration (EIA), Annual Energy Outlook 2012

Refracturing presents a promising strategy for addressing the characteristically steep decline rates of shale gas wells[3]. The core idea behind refracturing is to restimulate the reservoir such that it yields previously untapped hydrocarbons and improves the overall production profile of a well. Whether or not a refracture treatment will reinvigorate a shale gas well depends on a number of factors, including the characteristics of the reservoir and the initial completions design. Historically, refracture treatments have been applied predominantly to shale gas wells suffering from low production rates due to known suboptimal initial stimulations and completions. However, over the past years, the use of real-time microseismic hydraulic fracture mapping and other analytical tools has allowed operators to improve completions and stimulation designs, leading to a larger number of treated stages per well, meticulous stage selection, and increased fluid and proppant volumes[4]. Clearly, refracture treatments designed and performed under these revised insights can be expected to improve hydrocarbon recovery from unconventional reservoirs.

Moreover, Dozier et al.[5] argue that even wells with effective initial treatments have shown significant production improvements when restimulated after an initial period of production and partial reservoir depletion. On the one hand, the success of these workovers can be attributed to the fact that fracture conductivity is known to decrease over time as proppant packs become damaged or deteriorate with scale buildup during reservoir-pressure drawdown. Additional fracturing measures can address this issue, reestablish flow into the wellbore and reinvigorate a well's production profile. On the other hand, Dozier et al.[5] also point out that stress changes are known to occur around effective initial fractures as a result of reservoir depletion during production. These stress changes in turn lead to a *fracture reorientation*, which initiates new fractures along different azimuthal planes. Therefore, refracturing treatments performed at the right time can provide access to under- or unstimulated zones of the reservoir through these reoriented, newly created fractures. As such, well restimulations appear promising even for wells with effective initial treatments – especially in low permeability formations such as shale gas reservoirs.

The left image in Fig. 2 shows a horizontal wellbore and a typical fracture network induced by a wide-spaced hydraulic well stimulation. In contrast, the image on the right in Fig. 2 shows the same lateral wellbore and the surrounding reservoir after a refracture treatment. A comparison of the two images reveals that refracturing can add entirely new perforations to the existing fracture network and also extend previous fractures in new directions. Clearly, the enhanced fracture network has an increased surface area and reaches into previously unattainable areas of the reservoir.

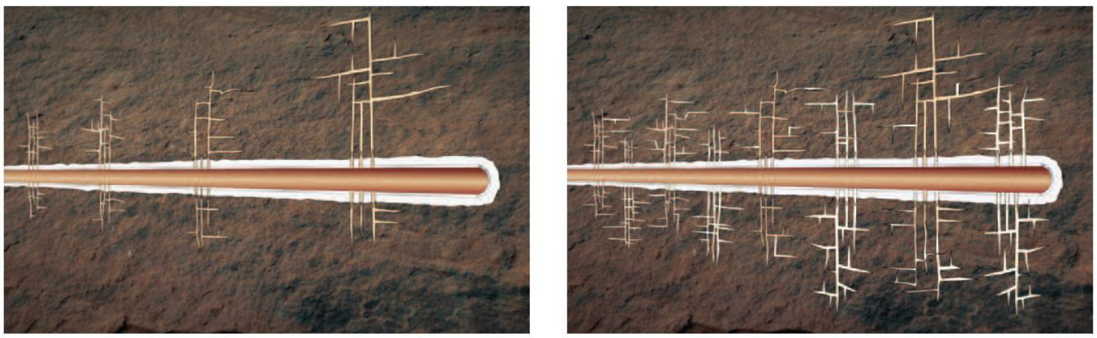

Fig. 2: A lateral well and the surrounding fracture network after initial well stimulation (left) and after a refracture treatment (right), Source: Allison and Parker[6]

Refracturing is known to cause a peak in the production rate that often matches up to 60% of the initial production peak, as seen in Fig. 3. In addition to restoring well productivity, refracture treatments present an opportunity to improve the completions design and can therefore alter long-term decline curves favorably by, for instance, enhancing fracture conductivity. Based on recent results, operators are increasingly confident that refracturing can enhance estimated ultimate recoveries (EUR) in excess of 30%, and thereby extend the expected lifespan of their shale wells beyond 20-30 years, especially when considering the possibility of multiple refracture treatments. This strategy seems particularly appealing given that refracturing an existing well generally costs less than half as much as completing a new well[3]; operators do not have to secure additional acreage, drill a well, or install pipelines for access to gathering systems. By reusing the existing infrastructure, refracturing also reduces surface disruption significantly, and therefore benefits the overall environmental impact of any field development project.

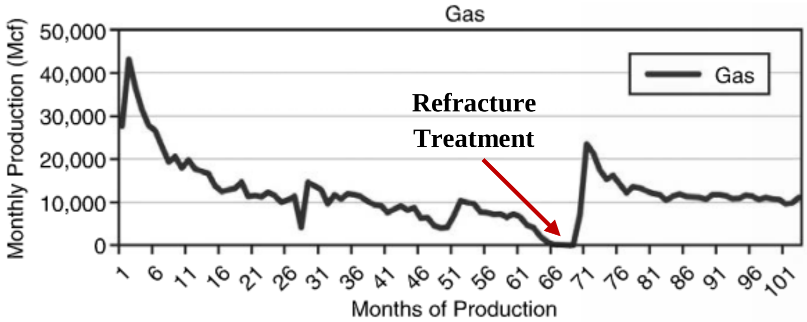

Fig. 3: Production profile of a refractured horizontal well in the Barnett Shale,

Source: Allison and Parker[6]

To this day, refracturing planning has received fairly little attention in the literature. One of the few contributions in this domain is a comprehensive report by Sharma[7], who addresses improved reservoir access through refracture treatments in greater detail. The author argues that refracturing has long been recognized as a successful way to restore production rates – particularly in low-permeability gas wells – by improving the productivity of previously unstimulated or understimulated reservoir zones. However, Sharma[7] also recognizes that the selection of candidate wells for refracturing is often very difficult based on the limited information available to decision-makers. The author claims that the timing of secondary reservoir stimulations, in particular, is critical for optimizing well performance. In the report, Sharma[7] proposes a number of dimensionless criteria to: (a) identify candidate wells for refracturing, and (b) determine the optimal refracture time in a well's lifespan. Among these criteria are a *well completions number* (indicating the quality of the initial completions), a *reservoir depletion number* (quantifying the extent of depletion around a particular well), a *production decline number* (reflecting the extent and quality of a reservoir) and a *stress reorientation number* (revealing the potential for additional fractures to propagate into underdepleted regions of the reservoir). In addition, the author proposes the use of dimensionless type curves to estimate the optimal time-window for refracture treatments.

Eshkalak et al.[8] focus on the economic feasibility of refracture treatments for horizontal shale wells. For an unconventional gas field consisting of 50 horizontal wells – all of which are considered candidates for refracturing – the authors calculate the net present value (NPV) and internal rate of return (IRR) for various refracturing scenarios that differ in terms of: (a) how many wells are refractured, (b) when wells are refractured, and (c) the given gas price forecast. The timing of the refracture treatments is specified in advance and the authors assume that the production increase due to restimulation is given by a fixed long-term refracturing efficiency factor. Based on the results of their analysis, Eshkalak et al. [8] conclude that refracturing shale gas wells makes economic sense over a wide range of price forecasts.

Tavassoli et al. [9] also address the refracturing planning problem. Motivated by the fact that – although refracturing strategies seem promising conceptually – merely 15-20% of all wells that have been refractured thus far achieved the desired performance targets, the authors develop a numerical, dual-permeability (matrix-fracture), two-phase (gas-water) simulation model. This model allows them to study the effect of different reservoir parameters (permeability, porosity) and operational decisions (initial fracture spacing, refracture timing) on refracturing performance. Their findings, too, suggest that the timing of a refracture job is absolutely crucial for success. In an attempt to provide some guidance for the optimal timing of refracturing treatments, the authors study typical shale gas well production decline curves in detail. They highlight the fact that typical shale well productivity curves evolve from steep, pronounced declines to more steady rates. Based on this analysis, the authors suggest that refracture treatments should be performed when the production decline rate falls below 10-15%, which – based on their numerical simulation studies – marks the point when gas production decline rates generally level off.

From the above we conclude that it is generally accepted that refracture timing is critical for optimizing the performance of any shale well. Yet, Lantz et al.[10] report that in practice, the time between the original completions stimulation and refracture treatments varies greatly. The authors describe a shale oil well refracturing program in the Bakken formation where some wells were refractured after 2 years while other wells produced for 3.5 years until they were restimulated. Previous work provides some guidelines or general heuristics as to when refracture treatments should be performed, but these indicators appear vague and often do not account for important economic factors, such as price forecasts or fracturing expenses.

Therefore, the objective of this work is to develop a modeling framework for planning optimal shale gas well refracture treatments.

2. GENERAL PROBLEM STATEMENT

The problem addressed in this paper can be stated as follows. We assume that a candidate shale gas well has been identified for refracturing. For this well, a long-term production forecast as well as the production profile after additional refracture treatments at any point in time over the planning horizon is given. A gas price forecast along with expenses for drilling, fracturing, completions and refracturing operations are also given.

The problem is to determine: (a) whether or not the well should be refractured, (b) how often the well should be refractured over its entire lifespan, and (c) when exactly the refracture treatments should be scheduled. The objective is to maximize either: (a) the estimated ultimate recovery (EUR) of the well, or (b) the net present value (NPV) of the well development project.

This paper is organized as follows. First, we present a continuous-time nonlinear programming (NLP) model to determine whether or not a shale gas well should be refractured, and when to schedule the refracture treatment. The NLP model relies on the assumption that the well productivity profile – prior to and after a refracture treatment – can be predicted by a decreasing power function of time. For this purpose we propose an effective forecast function that mimics real-life curves. In the following section we extend the proposed framework to allow for multiple refracture treatments and present a discrete-time mixed-integer linear programming (MILP). In this context, we review three alternative model formulations and explore their trade-offs in terms of model sizes and computational performance. Finally, we apply the discrete-time MILP model to two case studies to demonstrate the value of optimization for refracturing planning applications.

3. CONTINUOUS-TIME REFRACTURING PLANNING MODEL

Typically, the productivity curve of an ordinary shale gas well can be captured using a decreasing power function of time as stated in Eq. (1). Fig. 4 shows the fitness of such a function to forecasted production data provided by the EQT Corporation – a major shale gas producer in the Appalachian Basin (United States).

$$p(t) = k \cdot t^{-a} \qquad t \geq 1 \tag{1}$$

In Eq. (1) the productivity $p(t)$ is commonly specified in terms of MMscf/month, k is a parameter representing the initial production peak observed during the first month after turning a well in line, and $a > 0$ is the exponent representing the steepness of the production decline. We note that the productivity function $p(t)$ is only defined for $t \geq 1$. By our convention, we assume that time t = 0 corresponds to the beginning of drilling and completions operations, and that the well is ready to produce gas exactly one month later (i.e., at t = 1).

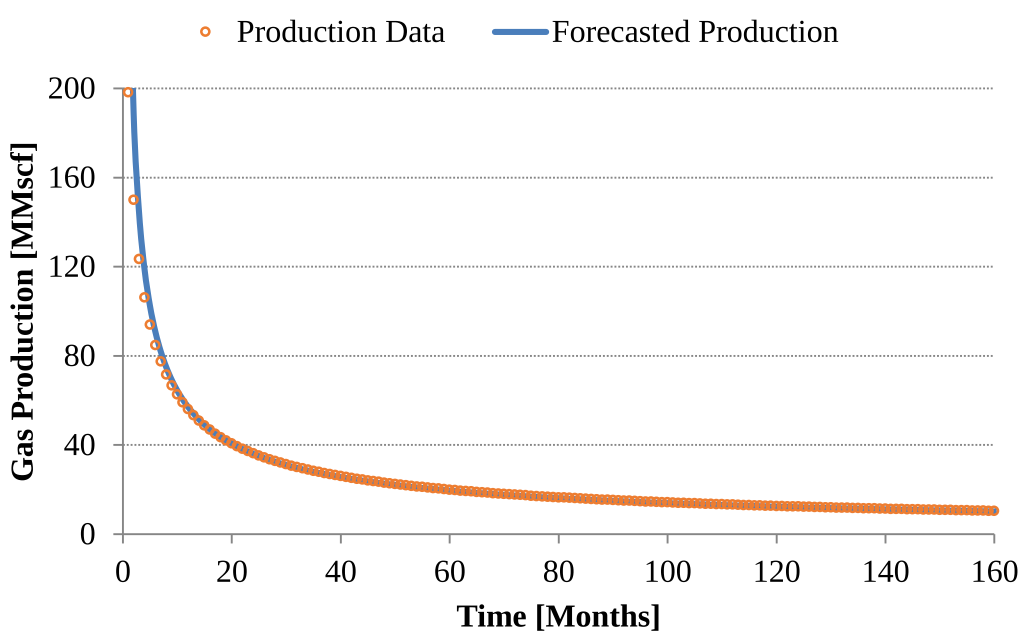

Fig. 4. *Comparison of real production forecast data and a fitted power function for a shale gas well*

While a shale gas well is being refractured, it does not produce any gas. We refer to this as the refracuring period rt. Once the refracture treatment has been completed and the well is turned in line again, a new peak in gas production is observed. Generally, this secondary production peak represents a fraction of the original peak and depends strongly on the characteristics of the reservoir, the refracturing technique and the original completions design. In this work we assume that the secondary peak can be expressed as $r = \beta \cdot k$, with typically $0.50 \leq \beta \leq 0.80$. Moreover, the production decline after refracturing follows a new decline curve, which is often steeper than the original decline following the original completions[9]. Motivated by real world data, we assume that the steepness of the productivity decline after refracturing (i.e., the magnitude of the exponent in the power function) increases linearly with the time between the original completions and the refracturing operation (namely, *trf*). On the other hand, given that the refracture operation can affect original fractures either favorably or unfavorably, the productivity of the original fractures is multiplied with the factor γ. In practice, the parameter γ needs to be specified in close coordination with completions design engineers, geologists and reservoir engineers, who are most familiar with the initial completions design as well as the particular reservoir characteristics. As a result, the productivity curve after refracturing can be represented by the function given in Eq. (2).

$$p(t) = \gamma \cdot k \cdot t^{-a} + r \cdot \left(t - trf - rt\right)^{-a-b \cdot trf} \qquad t \geq trf + rt + 1 \tag{2}$$

The variable *trf* is the time when refracturing starts (in months, after the original completions operation), γ is the factor that accounts for the increase or decrease in productivity of the original fractures, and b is the coefficient capturing the increase of the decline steepness after refracturing. Finally, we can express the productivity of a shale gas well before, during and after having been refractured using the function in Eq. (3).

$$p(t) = \begin{cases} k \cdot t^{-a} & 1 \leq t \leq trf \\ 0 & trf \leq t \leq trf + rt + 1 \\ \gamma \cdot k \cdot t^{-a} + r \cdot \left(t - trf - rt\right)^{-a-b \cdot trf} & trf + rt + 1 \leq t \leq T \end{cases} \tag{3}$$

In Fig. 5 we plot the function in Eq. (3) for different refracture start dates. We assume that a refracturing operation takes one month and that the resulting secondary peak (parameter r) is independent of the timing of the well restimulation. The latter assumption is supported by the work of Tavassoli et al[9].

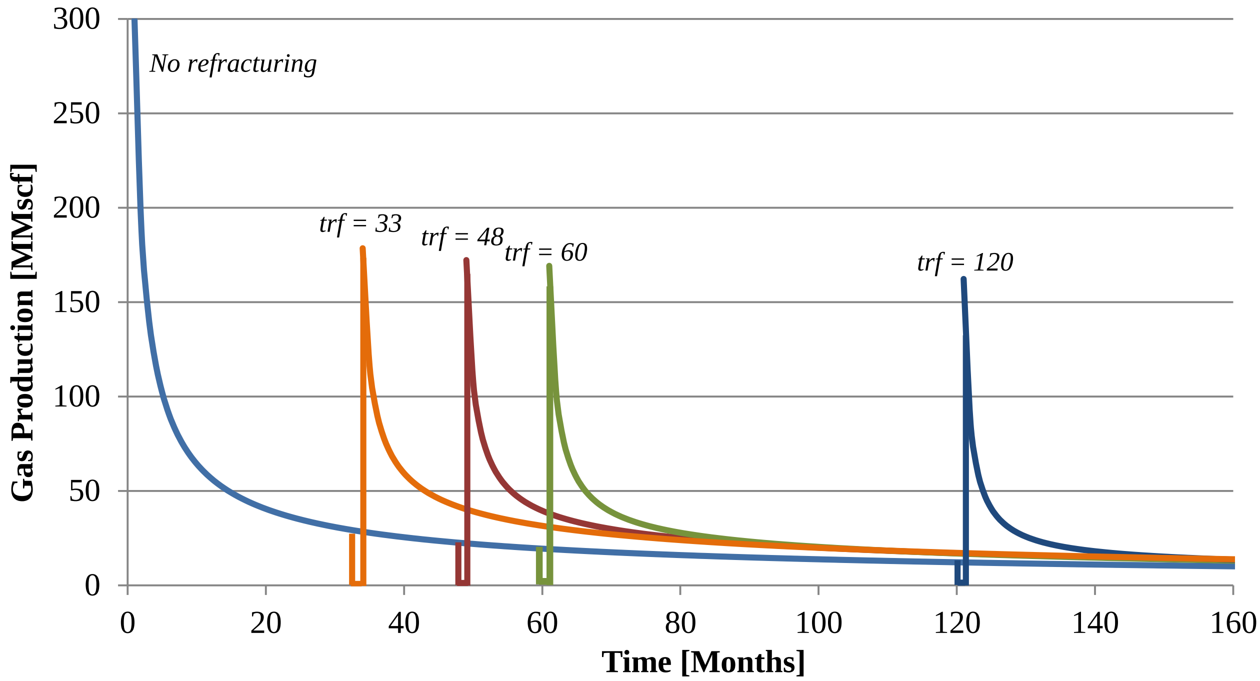

Fig. 5. *Productivity curves of a shale gas well for different refracture start dates (trf)*

To determine the total amount of gas that can be recovered from a shale gas well that has been refractured, we can integrate function (3) from $t = 1$ to $t = T$, where T represents the expected productive lifespan of the well. This key indicator of any shale gas well is usually referred to as the estimated ultimate recovery (EUR).

$$EUR(trf) = \frac{k}{1-a} \cdot \left[trf^{1-a} - 1 \right] + \frac{\gamma \cdot k}{1-a} \cdot \left[T^{1-a} - \left(trf + rt + 1 \right)^{1-a} \right] + \frac{r}{1-a-b \cdot trf} \cdot \left[\left(T - trf - rt \right)^{1-a-b \cdot trf} - 1 \right] \tag{4}$$

The EUR function in Eq. (4) assumes that: (1) $a \neq 1$, and (2) $a + b\ trf \neq 1$. To identify the optimal time to refracture a well such that the EUR is maximized, we propose a continuous-time nonlinear optimization model as in Eq. (5).

$$\begin{aligned} \max \quad & EUR(trf) = \frac{k}{1-a} \cdot \left[trf^{1-a} - 1 \right] + \frac{\gamma \cdot k}{1-a} \cdot \left[T^{1-a} - \left(trf + rt + 1 \right)^{1-a} \right] + \\ & \qquad \frac{r}{1-a-b \cdot trf} \cdot \left[\left(T - trf - rt \right)^{1-a-b \cdot trf} - 1 \right] \\ \text{s.t.} \quad & 1 \leq trf \leq T - rt - 1 \end{aligned} \tag{5}$$

This optimization model presents a singularity when $trf = (1 - a) / b$ for $1 \le (1 - a) / b \le T - rt - 1$. When this is the case, the denominator in the third term in Eq. (5) equals zero, leading to a division by zero. This explains why local and global solvers such as MINOS, CONOPT, BARON, COUENNE or LINDOGLOBAL[12] will oftentimes fail to converge to the optimal solution. For this reason, we propose to solve the problem in Eq. (5) as two separate optimization problems by dividing the planning horizon into two domains. First, we solve for $1 \le trf \le (1-a)/b-\varepsilon$, where ε is a small tolerance:

$$
\begin{aligned}
\max \quad & EUR(trf) = \frac{k}{1-a}\cdot\left[trf^{1-a}-1\right]+\frac{\gamma\cdot k}{1-a}\cdot\left[T^{1-a}-\left(trf+rt+1\right)^{1-a}\right]+ \\
& \qquad \frac{r}{1-a-b\cdot trf}\cdot\left[\left(T-trf-rt\right)^{1-a-b\cdot trf}-1\right] \\
\text{s.t.} \quad & 1 \le trf \le (1-a)/b-\varepsilon
\end{aligned}
\tag{6}
$$

Next, we solve for $(1-a)/b+\varepsilon \le trf \le T-rt-1$:

$$
\begin{aligned}
\max \quad & EUR(trf) = \frac{k}{1-a}\cdot\left[trf^{1-a}-1\right]+\frac{\gamma\cdot k}{1-a}\cdot\left[T^{1-a}-\left(trf+rt+1\right)^{1-a}\right]+ \\
& \qquad \frac{r}{1-a-b\cdot trf}\cdot\left[\left(T-trf-rt\right)^{1-a-b\cdot trf}-1\right] \\
\text{s.t.} \quad & (1-a)/b+\varepsilon \le trf \le T-rt-1
\end{aligned}
\tag{7}
$$

It should be noted that it is very unlikely that the optimal value for *trf*, i.e., the optimal time to refracture a well, matches the singular value $(1 - a) / b$ at the optimum. Generally, $(1 - a) / b > T$, which implies that the singular value for *trf* lies outside the feasible region and far beyond the expected lifespan of an ordinary shale gas well.

Fig. 6 shows the relationship between the timing of the refracture treatment *trf* and the EUR for different steepness values *a* based on the function in Eq. (4). All other parameters remain the same. It can be observed that refracturing can raise the *EUR* up to 22.5%, depending on the productivity curve. We also note that the wells featuring higher values of *a* (i.e., steeper declines) should be refractured later in their lifespan, achieving lower increases in the well reserves.

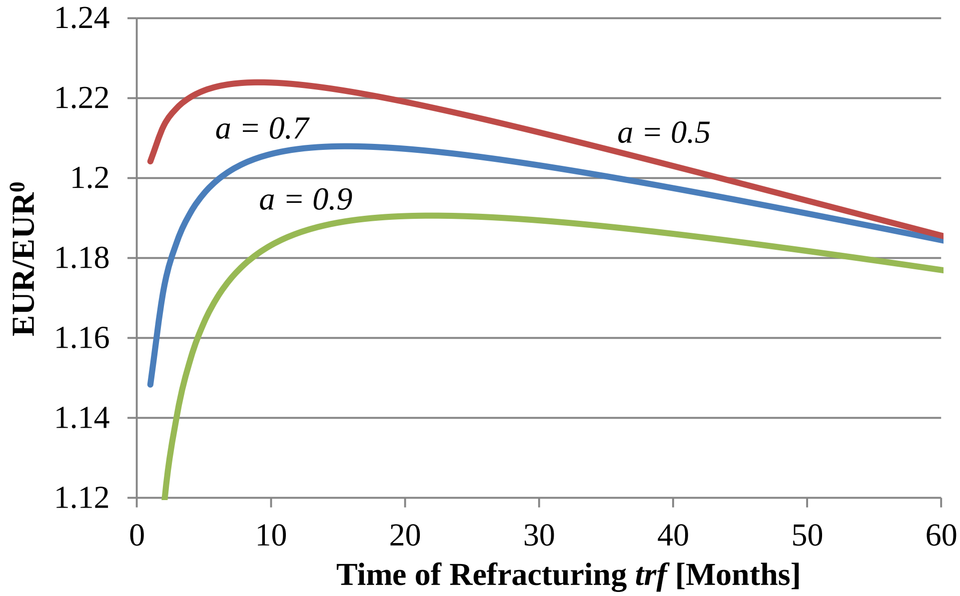

Fig. 6. *EUR ratios with and without refracturing with regards to the time of refracturing*

4. MULTIPERIOD REFRACTURING PLANNING MODEL

The continuous-time NLP model presented in the previous section is particularly useful for identifying the optimal time for refracturing a typical shale gas well so as to maximize its expected ultimate recovery (EUR). In practice, however, the NLP model has the following shortcomings: (a) it is not suitable for planning multiple refracture treatments over the expected lifespan of the well, (b) it does not allow for the evaluation of economic objective functions, such as the net present value (NPV), and (c) it only admits forecasted production decline curves strictly following the fundamental power function given by Eq. (3). To overcome these limitations, we also present a discrete-time, multiperiod mixed-integer linear programming (MILP) model that – unlike the continuous model – is capable of planning multiple refracturing operations while accounting for an economic evaluation of the well development project.

We assume that the planning horizon has been discretized into a set of time periods $t \in T$, usually months. The decision-maker is considering a candidate number of refracture treatments $i \in I_0$ that are ordered chronologically. We note that the set I_0 explicitly contains the zero-element, i.e. $I_0 = \{i_0\} \cup I = \{i_0; i_1; i_2;...\}$. The practical interpretation of this element is that the well may not be refractured at all. Generally, we recommend to set $|I| = 2$ to 3 for a planning horizon of 10 years, even though some researchers[11] argue that up to five refracture treatments may be performed over the expected lifetime of a shale gas well. Moreover, we advise to set $|T|$ = 120 to 360 – corresponding to 10 to 30 years. Next, we introduce the binary variable $x_{i,t}$ which is active if the well is refractured for the i-th time in time period t. Then, the following equations hold.

$$\sum_{t \in T} x_{i,t} \leq 1 \qquad \forall i \in I \tag{8}$$

$$x_{i,t} \leq \sum_{\tau < t - rt} x_{i-1,\tau} \qquad \forall i \in I, t \in T, i > 1 \tag{9}$$

Eq. (8) states that a well cannot be refractured for the i-th time more than once. In fact, the formulation allows the well not to be refractured at all since this is a true degree of freedom in practice. Moreover, Eq. (9) ensures that if a well is refractured for the i-th time in time period t, then it has to have been refractured for the (i-1)-th time in one of the previous time periods $\tau < t - rt$, where rt is the number of time periods it takes to restimulate the well.

Production profile

From the analysis of shale gas productivity curves before, during, and after a refracture treatment presented in Section 3, we can state that prior to any refracturing operation, the production curve obeys a decreasing power function as given in Eq. (1). Hence, the gas production in time period t can be bounded from above as follows.

$$P_t \leq k \cdot t^{-a} + \hat{k} \cdot \sum_{\tau \leq t} x_{i1,\tau} \qquad \forall t \in T \tag{10}$$

We note that constraint (10) is relaxed if the well has been refractured once or more often by time period t. $\hat{k}$ is an overestimator of the new production peak we expect after a refracture treatment. Usually, we set $\hat{k} = k$. During the refracturing procedure itself, the well will not produce any gas. Therefore, during the rt time periods it takes to restimulate the well, the production is set to zero by constraint (11).

$$P_t \leq \max(k, \hat{k}) \cdot \left(1 - \sum_{\tau = t - rt + 1}^{t} \sum_{i \in I} x_{i,\tau} \right) \qquad \forall t \in T \tag{11}$$

In fact, Eq. (11) states that if the well was refractured in any of the previous $rt-1$ time periods, then the production rate in time period t must be zero.

Once a well has been refractured, it becomes more challenging to model its production rate, since the well's productivity depends on precisely how often and also when a restimulation was last performed. For this purpose, we introduce the binary decision variable $y_{i,t} \in [0,1]$ (can be treated as a continuous variable) that is meant to become active (i.e., equal to one) if by the end of time period t the well has been refractured i times. This distinction is important because in any time period t the well may have been refractured i times even though the last refracturing operation occurred in a previous time period $\hat{t} < t$. We derive the following mixed-integer constraints through propositional logic[14] to capture the relation between the decision variables $x_{i,t}$ and $y_{i,t}$ by using their equivalent Boolean variables.

$$x_{i,t} \quad \Rightarrow \quad y_{i,t} \qquad \forall i \in I_0, t \in T \tag{12}$$

Eq. (12) states that if the well is refractured for the i-th time in time period t, then the well has been refractured i times by the end of that period. This logic statement can be expressed through Eq. (13).

$$x_{i,t} \le y_{i,t} \qquad \forall i \in I_0, t \in T \tag{13}$$

Next, we argue that if the i-th refracturing is the last that occurred as of the end of time period t, i.e., the decision variable $y_{i,t}$ is active, then in one of the previous time periods the well had to have been refractured for the i-th time.

$$y_{i,t} \quad \Rightarrow \quad x_{i,t1} \vee x_{i,t2} \vee x_{i,t3} \vee \ldots \vee x_{i,t} \qquad \forall i \in I_0, t \in T \tag{14}$$

The corresponding mixed-integer constraint is given by Eq. (15).

$$y_{i,t} \le \sum_{\tau \le t} x_{i,\tau} \qquad \forall i \in I_0, t \in T \tag{15}$$

Indeed, if by the end of time period t-1 the well has been refractured a total of i times, i.e., the decision variable $y_{i,t-1}$ is active, but in the subsequent time period t the decision variable $y_{i,t}$ is no longer active, then the well must have been refractured for the (i+1)-th time in this time period t, i.e., the decision variable $x_{i+1,t}$ has to be active.

$$y_{i,t-1} \quad \wedge \quad \neg y_{i,t} \quad \Rightarrow \quad x_{i+1,t} \qquad \forall i < |I_0|, t > 1 \tag{16}$$

Eq. (16) matches exactly with Eq. (17) in mixed-integer form.

$$y_{i,t} \geq y_{i,t-1} - x_{i+1,t} \qquad \forall i < |I_0|, t > 1 \tag{17}$$

Finally, we ensure that in any time period only a single number of refracture operations i may have occurred previously.

$$\sum_{i \in I_0} y_{i,t} = 1 \qquad \forall t \in T \tag{18}$$

Next, we propose three alternative formulations for capturing the productivity profile of a shale gas well after it has been refractured once or more often. In Section 5.2 we study the computational performance of these formulations.

Big-M Formulation

Given the decision variables $x_{i,\hat{t}}$ and $y_{i,t}$ we can impose an upper bound on the production of the shale gas well after refracturing, as stated by constraint (19).

$$P_t \leq \gamma^i \cdot k \cdot t^{-a} + \beta_{i,\hat{t}} \cdot r \cdot \left(t - \hat{t} - rt + 1\right)^{-a-b\cdot\hat{t}} + \hat{k} \cdot \left(2 - y_{i,t} - x_{i,\hat{t}}\right) \qquad \forall i \in I, t \in T, \hat{t} \leq t - rt \tag{19}$$

Constraint (19) is a key part of the model and deserves to be analyzed in detail. It is an upper bound only imposed on the gas production in time period t when – at the end of time period t – the well has been refractured i times ($y_{i,t}$ = 1) and this i-th refracturing operation occurred in time period $\hat{t} < t - rt$ ($x_{i,\hat{t}}$ = 1). The production of the well during time period t is composed of two parts: (a) the contribution of the original fractures, which is increased or decreased by the factor γ (normally $\gamma < 1$) every time a new refracture treatment is performed, and (b) the contribution of newly induced fractures. In the latter case, it is assumed that the first refracturing operation yields a peak of magnitude r (see Section 3 for details), and every further refracture treatment yields a smaller peak derived from multiplying the previous peak with the factor $\beta_{i,\hat{t}} < 1$. Hence, the parameter $\beta_{i,\hat{t}}$ depends on two factors: (a) how often the well has been refractured (index i), and (b) when the last refracture treatment occurred (index $\hat{t}$). For simplicity, one may assume that $\beta_{i,\hat{t}} = \beta_i$, which implies that every additional refracture treatment yields the same reduction in the post-refracture production peak, regardless of when it is performed. Similar to the continuous model, the corresponding production curves' declines are steeper the later the refracturing is performed, which is driven by the exponent $(-a - b\,\hat{t})$. We refer to Eq. (19) as the *big-M formulation* (BMF).

Disjunctive Formulation: Standard Hull-Reformulation

Given the decision variables $x_{i,\hat{t}}$ and $y_{i,t}$ we can also introduce an additional binary variable $z_{i,t,\hat{t}}$. This variable is active if and only if at the end of time period t the well has been refractured a total of i times ($y_{i,t}$ =1) and the last refracturing occurred in time period $\hat{t}$ ($x_{i,\hat{t}}$ =1). This binary variable is defined by the following logic.

$$y_{i,t} \wedge x_{i,\hat{t}} \Rightarrow z_{i,t,\hat{t}} \qquad \forall i \in I_0, t \in T, \hat{t} \le t - rt \tag{20}$$

We can easily transform Eq. (20) into the following mixed-integer constraint using propositional logic[14].

$$y_{i,t} + x_{i,\hat{t}} \le z_{i,t,\hat{t}} + 1 \qquad \forall i \in I_0, t \in T, \hat{t} \le t - rt \tag{21}$$

In addition, we include the reverse logic statement as well.

$$z_{i,t,\hat{t}} \Rightarrow y_{i,t} \wedge x_{i,\hat{t}} \qquad \forall i \in I_0, t \in T, \hat{t} \le t - rt \tag{22}$$

This, too, can easily be transformed into the following two constraints:

$$z_{i,t,\hat{t}} \le y_{i,t} \qquad \forall i \in I_0, t \in T, \hat{t} \le t - rt \tag{23}$$

$$z_{i,t,\hat{t}} \le x_{i,\hat{t}} \qquad \forall i \in I_0, t \in T, \hat{t} \le t - rt \tag{24}$$

The advantage of having introduced the binary variable $z_{i,t,\hat{t}}$ is that we can derive a disjunctive model for the key production constraint.

$$\vee_{i \in I_0, \hat{t} \in 1..t-rt} \left[\begin{array}{c} z_{i,t,\hat{t}} \\ P_t \le \tilde{\gamma}_i \cdot k \cdot t^{-a} + \tilde{\beta}_{i,\hat{t}} \cdot r \cdot \left(t - \hat{t} - rt + 1\right)^{-a-b\cdot\hat{t}} \end{array} \right] \qquad \forall t \in T \tag{25}$$

$$\underline{\vee}_{i \in I_0, \hat{t} \in 1..t-rt} \quad z_{i,t,\hat{t}} \qquad \forall t \in T \tag{26}$$

It is important to note that in the formulation above, $\tilde{\gamma}_i$ and $\tilde{\beta}_{i,\hat{t}}$ are *parameters*. In particular, we clarify that $\tilde{\gamma}_{io} = 1$ and $\tilde{\beta}_{i0,\hat{t}} = 0$. Moreover, we highlight the fact that the binary variable $z_{i,t,\hat{t}}$ can be declared as a *continuous variable* due to constraints (21),(23),(24), which enforce integrality for 0-1 values of $x_{i,t}$ and $y_{i,t}$. As outlined by Grossmann and Trespalacios[15] we use the Hull-Reformulation (HR) to transform disjunctions (25)-(26) into the set of mixed-integer constraints (27)-(29).

$$P_{i,t,\hat{t}} \leq \left(\tilde{\gamma}_i \cdot k \cdot t^{-a} + \tilde{\beta}_{i,\hat{t}} \cdot r \cdot \left(t - \hat{t} - rt + 1 \right)^{-a-b\cdot\hat{t}} \right) \cdot z_{i,t,\hat{t}} \qquad \forall i \in I, \hat{t} \in 1 \ldots t-rt, t \in T \tag{27}$$

$$P_t = \sum_{i \in I_0} \sum_{\hat{t}=1}^{t-rt} P_{i,t,\hat{t}} \qquad \forall t \in T \tag{28}$$

$$\sum_{i \in I_0} \sum_{\hat{t}=1}^{t-rt} z_{i,t,\hat{t}} = 1 \qquad \forall t \in T \tag{29}$$

We refer to constraints (27)-(29) as the *Standard Hull-Reformulation* (SHR).

Disjunctive Formulation: Compact Hull-Reformulation

In this particular case it is possible to derive a more compact reformulation of the disjunctive model. For this purpose we sum up constraint (27) over all $\hat{t} \in 1 \ldots t - rt$ for every time period $t \in T$ and every number of candidate refracture operations $i \in I_0$. Also, we introduce the partially disaggregated variable $P_{i,t} = \sum_{\hat{t}=1}^{t-rt} P_{i,t,\hat{t}}$. The result is shown in Eqs. (30)-(31).

$$P_{i,t} \leq \sum_{\hat{t}=1}^{t-rt} \left(\tilde{\gamma}_i \cdot k \cdot t^{-a} + \tilde{\beta}_{i,\hat{t}} \cdot r \cdot \left(t - \hat{t} - rt + 1 \right)^{-a-b\cdot\hat{t}} \right) \cdot z_{i,t,\hat{t}} \qquad \forall i \in I_0, t \in T \tag{30}$$

$$P_t = \sum_{i \in I_0} P_{i,t} \qquad \forall t \in T \tag{31}$$

$$\sum_{i \in I_0} \sum_{\hat{t}=1}^{t-rt} z_{i,t,\hat{t}} = 1 \qquad \forall t \in T \tag{32}$$

The key advantage is that the triple-indexed disaggregated variables $P_{i,t,\hat{t}}$ can be replaced by the double-indexed variables $P_{i,t}$, hence reducing the total number of decision variables. Also, the formulation in

Eqs. (30)-(32) involves fewer constraints. In fact, the proposed formulation can be improved even further by summing up constraint (30) over all $i \in I_0$ in every time period $t \in T$.

$$P_t \leq \sum_{i\in I_o}\sum_{\hat{t}=1}^{t-rt}\left(\tilde{\gamma}_i \cdot k \cdot t^{-a} + \tilde{\beta}_{i,\hat{t}} \cdot r \cdot \left(t-\hat{t}-rt+1\right)^{-a-b\cdot\hat{t}}\right)\cdot z_{i,t,\hat{t}} \qquad \forall t \in T \tag{33}$$

$$\sum_{i\in I_0}\sum_{\hat{t}=1}^{t-rt} z_{i,t,\hat{t}} = 1 \qquad \forall t \in T \tag{34}$$

Now the formulation does not involve any disaggregated variables or the corresponding constraints, and hence we refer to the aggregated Eqs. (33)-(34) as the *Compact Hull-Reformulation* (CHR). For more details regarding the CHR we refer to the Appendix.

Finally, we note that in certain cases, when rigorous reservoir simulation tools are available, the forecasted production profile after any number of refracture treatments can be directly specified as a parameter, namely $Q_{i,t,\hat{t}}$. This parameter captures the predicted production of the well in time period *t* when the well has been refractured *i* times, and the last refracture treatment started in time period $\hat{t} < t - rt$. If so, Eqs. (19), (25), (27) and (30) turn into Eqs. (35)-(38), respectively, which represents a much more compact formulation.

$$P_t \leq Q_{i,t,\hat{t}} + \hat{k}\cdot\left(2 - y_{i,t} - x_{i,\hat{t}}\right) \qquad \forall i \in I, t \in T, \hat{t} \leq t - rt \tag{35}$$

$$\vee_{i\in I_0,\hat{t}\in 1\ldots t-rt}\begin{bmatrix} z_{i,t,\hat{t}} \\ P_t \leq Q_{i,t,\hat{t}} \end{bmatrix} \qquad \forall t \in T \tag{36}$$

$$P_{i,t,\hat{t}} \leq Q_{i,t,\hat{t}} \cdot z_{i,t,\hat{t}} \qquad \forall i \in I_o, \hat{t} \in 1\ldots t-rt, t \in T \tag{37}$$

$$P_{i,t} \leq \sum_{\hat{t}=1}^{t-rt} Q_{i,t,\hat{t}} \cdot z_{i,t,\hat{t}} \qquad \forall i \in I_0, t \in T \tag{38}$$

Objective Function

The intended goal of the multiperiod model is to maximize the net present value (NPV) of a shale gas well development project. Therefore, the objective function involves positive terms accounting for natural gas sales, as well as negative terms related to drilling, fracturing and refracturing expenses. All these terms are discounted back to the present time with a monthly discount rate d. Drilling costs (DC) and completions costs (CC) are considered to be expenditures at the present time. The unit shale gas profit (gp_t) is the difference between the unit gas price and the production costs, while RC is the total cost of a single refracture treatment. Hence, the objective function of the MILP is given by Eq.(39).

$$\max \quad NPV = \sum_{t \in T} (1+d)^{-t} \cdot \left[P_t \cdot gp_t - RC \cdot \sum_{i \in I} x_{i,t} \right] - DC - CC \tag{39}$$

5. COMPUTATIONAL RESULTS

We apply the proposed discrete-time MILP model to two case studies. Our first example is a typical shale gas well development planning problem with hypothetical data, whereas the second example is based on simulation results presented by Tavassoli et al. [9] who rely on real-world data from a Barnett shale well.

5.1. Example 1

Given a 10 year planning horizon, we assume that the decision-maker is considering a total of two possible refracture treatments for a particular well development project. Production forecasts with and without refracture treatments are given and factored into the analysis. It is assumed that every additional well stimulation takes about one month during which the well cannot produce any gas. It is also assumed that original drilling, fracturing and completions expenses amount to 3 million USD, whereas every additional refracturing operation costs 800,000 USD. It is important to note that the optimal refracturing strategy is very sensitive to the assumed restimulations costs, which can vary greatly depending on the completions design. In a recent publication, several operators reveal that they expect to spend between 12.5 % and 20.0 % of the initial well development cost for every refracture treatment.[13] We decide to take a more conservative approach here and assume that the refracturing procedure costs nearly 30 % of the initial completions expenses. The monthly discount rate d to evaluate the project is 1 %. Lastly, we assume a fixed specific profit of \$ 1.5 per produced Mscf (\$ 0.05 per produced m^3) over the entire planning horizon. All other model parameters are specified in Table 1. The decision-maker's objective is to maximize the net present value of the well development project.

Model Parameters	Parameter Notation	Values	Units
Initial well production rate	k	299.4	[MMscf/month]
Production decline exponent	a	0.6674	[-]
Post-refracturing production rate	r	120	[MMscf/month]
Post-refracturing decline change	b	0.0005	[1/month]
Time required for refracturing	rt	1	[months]
Initial fractures contribution	γ	1	[-]

Table 1. *Model parameter specifications for Example 1.*

We solve the MILP model for this problem to zero optimality gap, and identify a refracturing strategy that yields a positive NPV of 765,434 USD (for all computational details we refer to Section 5.2). The solution reveals a single refracturing operation, scheduled exactly 26 months after the original well stimulation. Our results suggest that this single refracture treatment allows the operator to increase the EUR from 3,696 MMscf (104.4 x 10^6 m^3) to 4,609 MMscf (130.2 x 10^6 m^3); a remarkable 25% increase over the given planning horizon. Without the well-restimulation, the projected NPV reduces to 625,664 USD.

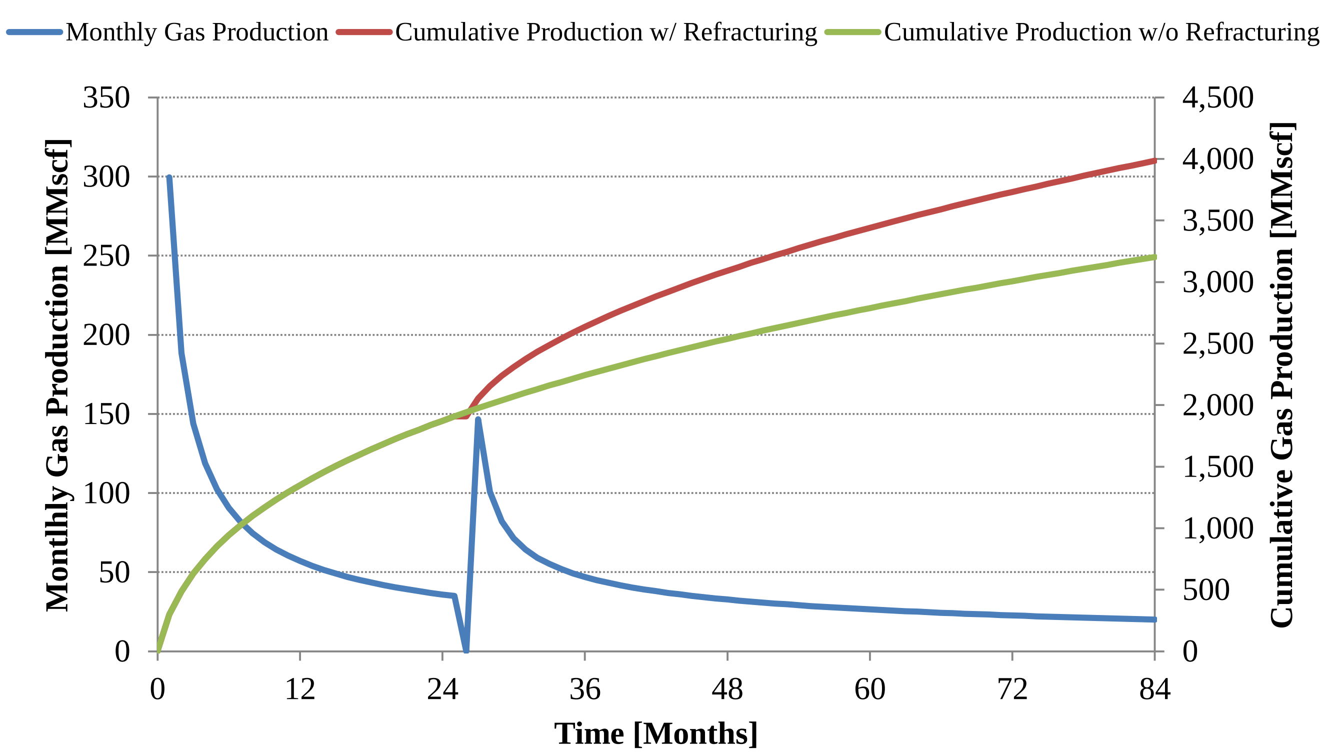

Fig. 7. *Optimal production curve of a shale gas well studied in Example 1*

The NLP model presented in Section 3 can also be applied to this example – as long as only one single refracture treatment is allowed over the given planning horizon. In this case the objective function needs to be replaced by the maximization of the expected ultimate recovery (EUR) since, as outlined previously, the NLP model is not designed for economic objective functions. Here, the NLP model reveals that the best time for a single refracture treatment is *trf* = 29.72 months. This solution is obtained in less than one second using BARON 16.3 in GAMS 24.2.2.[12] We find that using the MILP model yields a similar solution (*trf* = 28) when the EUR is maximized – rather than the NPV. The slight difference between both solutions can be attributed to the conversion of the continuous to the discrete time scale. We also note that the singular value for the variable *trf* in the NLP is (1 – a) / b = (1-0.6674)/0.0005 = 665.2 months, much larger than the extent of the planning horizon.

5.2. Comparison of Different Formulations applied to Example 1

In this section we compare the three alternative MILP formulations proposed in Section 4, namely the *Big-M Formulation (BMF)*, the *Standard Hull-Reformulation (SHR),* and the *Compact Hull-Reformulation (CHR)* in terms of model size and computational performance. We note that all three formulations yield the exact same solution, as reported in the previous section. Table 2 summarizes selected computational statistics for all three formulations when solving Example 1 using Gurobi 5.6.2 in GAMS 24.2.2[12] on an Intel i7, 2.93 Ghz machine with 8 GB RAM.

	BMF	**SHR**	**CHR**
Binary variables	240	360	360
Continuous variables	481	44,161	22,381
Constraints	15,603	89,163	67,383
Nodes	7,786	0	0
Solution time [seconds]	**255**	**22**	**9**

Table 2. *Computational statistics for the Big-M Formulation (BMF), the Standard Hull-Reformulation (SHR), and the Compact Hull-Reformulation (CHR) using Gurobi 5.6.2*[12].

Table 2 clearly shows that the BMF yields the smallest model size in terms of variables and constraints. However, out of the three proposed formulations it also requires the largest solution time (255 s). Despite the fact that the SHR leads to a significantly larger model, it takes less time to solve the same problem: merely 22 s. What is even more impressive is that Gurobi succeeds at solving the MILP problem to optimality at the root node, i.e., prior to branching on any discrete variable. Compared to the SHR, the CHR yields a reduced model size in terms of the number of continuous variables and constraints. As with the SHR, the problem is solved at the root node, but now it takes merely 9 s to obtain the global optimum. Table 3 summarizes the computational statistics of all three formulations when solving Example 1 using CPLEX 24.4.6 in GAMS 24.2.2[12] on an Intel i7, 2.93 Ghz machine with 8 GB RAM.

	BMF	**SHR**	**CHR**
Binary variables	240	360	22,140
Continuous variables	481	44,161	22,381
Constraints	15,603	89,163	67,383
Nodes	10,612	0	0
Solution time [seconds]	**64**	**12**	**11**

Table 3. *Computational statistics for the Big-M Formulation (BMF), the Standard Hull-Reformulation (SHR), and the Compact Hull-Reformulation (CHR) using CPLEX 24.4.6*[12].

Conceptually, the computational results for solving Example 1 using CPLEX 24.4.6[12] as depicted in Table 3 compare directly to those obtained by solving the problem using GUROBI 5.6.2[12]. However, it is interesting to note that the problem solves much faster using CPLEX, particularly for the BMF and SHR models. We also observe that the continuous linear programming (LP) relaxations of all three formulations are nearly identical. The fact that CPLEX and Gurobi solve the problem at the root node can be attributed to the structure of the SHR and CHR formulations, which allow the solvers to take advantage of added cutting planes, efficient heuristics and constraint propagation.

5.3. Example 2

In our second case study we rely on a numerical reservoir simulation model developed by Tavassoli et al.[9] to determine optimal refracturing strategies for a well development project. For this purpose we assume that an upstream operator has already decided to develop a particular shale gas well. The reservoir simulation model proposed by Tavassoli et al. [9] allows us to predict the well's production profile over a 30 year planning horizon based on real data from a Barnett shale well. Moreover, the model is capable of determining the well's production profile after refracture treatments induced 24, 36, 48, 60, or 72 months after the original well completions. However, unlike Tavassoli et al. [9], we assume that the well may potentially be restimulated *twice* over its lifespan. The production forecast after secondary refracture treatments is estimated based on the simulation results by Tavassoli et al.[9]. Through a number of case study variations, we show that our proposed refracturing planning model is capable of determining different optimal restimulation strategies, depending on what type of price forecast is given. As before, we assume that drilling, fracturing and completions expenses amount to 3 million USD, whereas every additional refracturing operation costs 800,000 USD and takes exactly one month. The monthly discount rate d is assumed to be 1 %.

Price Forecast with a Seasonal Pattern

Our initial example assumes a price forecast with an underlying seasonal trend pattern. For demonstration purposes we rely on historic Henry Hub spot price data to simulate such a price forecast. The resulting MILP model involves a total of 6,873 binary variables, 7,576 continuous variables, and 22,026 constraints. We note that the decision variables $y_{i,t}$ and $z_{i,t,\hat{t}}$ can be declared as continuous variables, which can result in an improved computational performance depending on the solver selection. The problem is solved to global optimality in less than 2 seconds using CPLEX 24.4.6[12] on an Intel i7, 2.93 Ghz machine with 8 GB RAM.

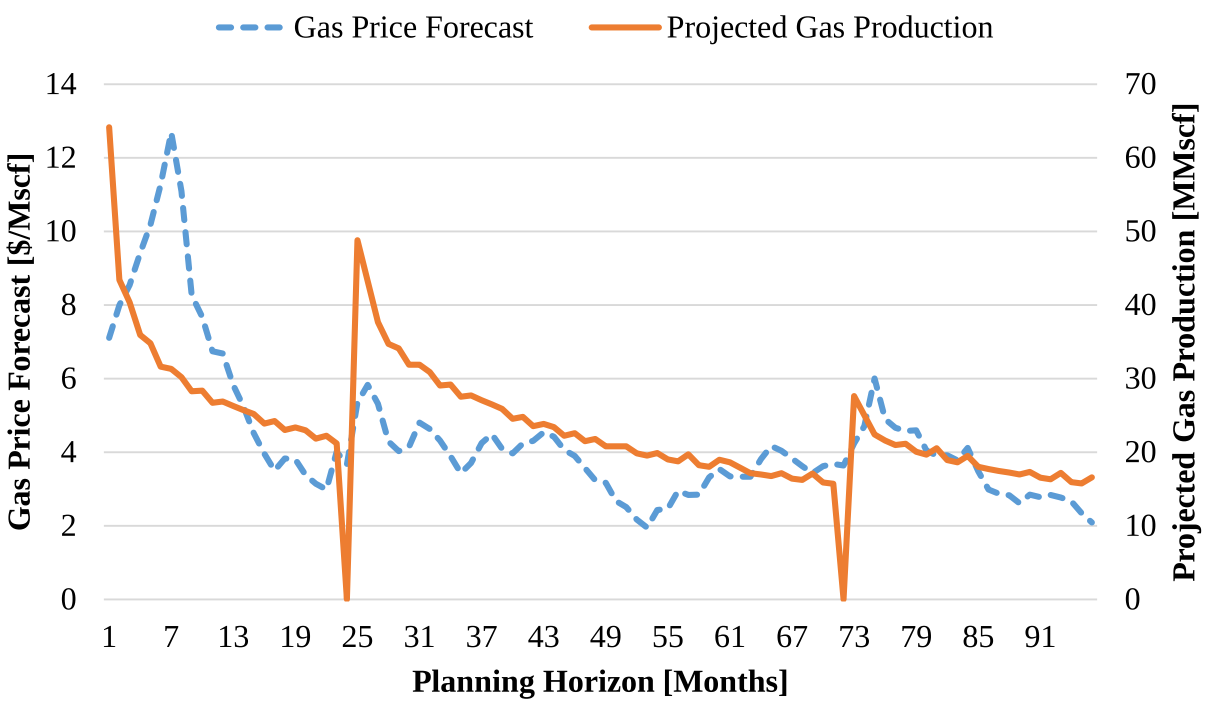

Fig. 8. *Optimal production curve for a shale gas well given a price forecast (refracture treatments scheduled after 24 months and 72 months respectively)*

The optimal solution we identify yields a positive NPV of 5.7 million USD. As shown in Fig. 8, the MILP optimizer proposes two refracturing treatments: one 24 months and the other 72 months after initial completions. A comparison of the given price forecast and the projected production profile in Fig. 8 suggests that both restimulations are scheduled such that they exploit price peaks in the forecast. Clearly, the given price forecast has a fundamental impact on the optimal well development strategy. Therefore, we also study two alternative future price forecasts assuming fewer stochastic price swings.

Upwards Trend Price Forecast with a Seasonal Pattern

We modify the underlying price forecast for the problem and assume an upwards trend price forecast with a seasonal pattern. This forecast is taken from the CME Group's Henry Hub natural gas futures quote in January 2016[16]. The size of the optimization problem and the solution time are the same as in the previous variation of the example.

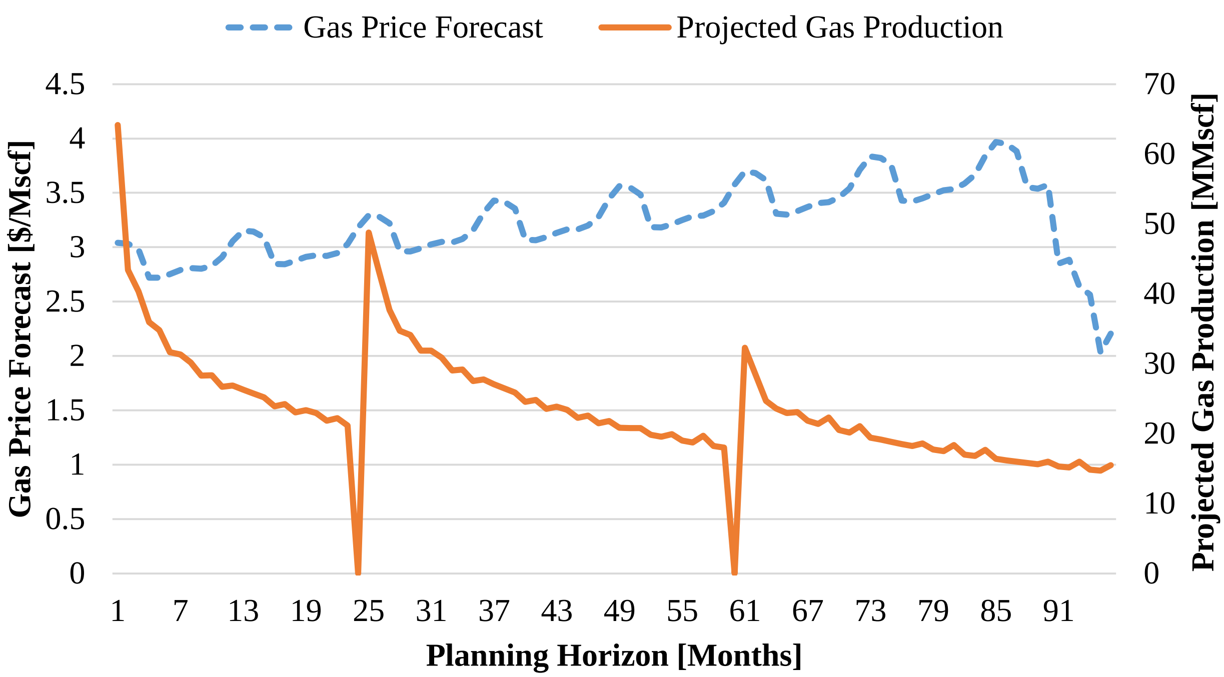

Fig. 9. *Optimal production curve for a shale gas well given an upwards trend price forecast (refracture treatments scheduled after 24 months and 60 months respectively)*

Given the price forecast seen in Fig. 9, the solution from the MILP model yields a positive NPV of 2.1 million USD. The decrease in well development profitability – compared to the previous variation of the example – is clearly due to a lower price forecast. However, in this case too, the solution suggests that a total of two refracturing treatments should be performed over the lifespan of the well: the first well restimulation should occur 24 months after well completions (as before) and the second one 3 years later (unlike 4 years before). Without additional refracturing treatments, the predicted NPV for this particular well development project diminishes to merely 1.6 million USD.

Downwards Trend Price Forecast with Seasonal Pattern

Finally, we modify the underlying price forecast for the problem once more and assume a downwards trend price forecast with a seasonal pattern. This forecast is entirely hypothetical but motivated by the CME Group's Henry Hub natural gas futures quotes[16]. As before, the size of the optimization problem and the solution time are the same as in the previous variation of the example.

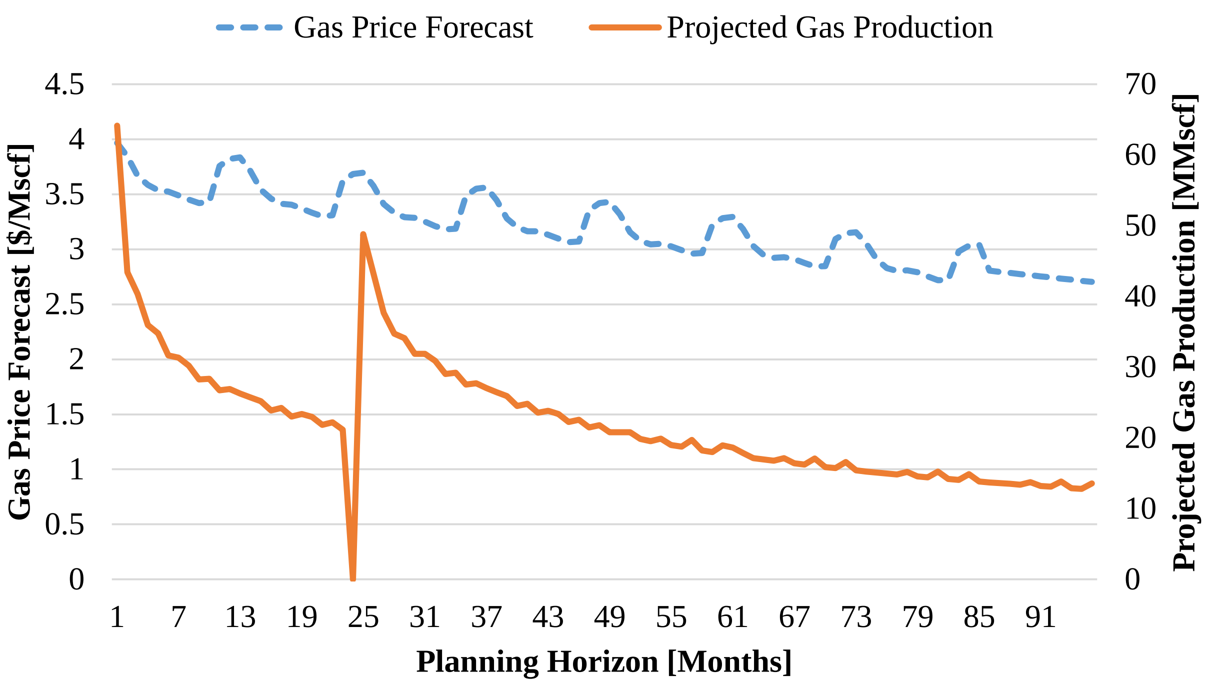

Fig. 10. *Optimal production curve for a shale gas well given a downwards trend price forecast (single refracture treatment scheduled after 24 months)*

Based on the revised price forecast shown in Fig. 10, the optimization yields a positive NPV for the well development project of 2.0 million USD. Despite the downward trend of the price forecast, the solution suggests that well development is economically favorable. However, in this particular case the solution shows that only a single refracture treatment should be performed, and it should occur two years into the planning horizon. Without this restimulation, the predicted NPV decreases to 1.5 million USD.

The above examples clearly demonstrate that price forecasts have a significant impact on optimal restimulation strategies – particularly on the frequency and timing of such measures. Hence, we argue that well development economics – and price forecasts in particular – need to be taken into account whenever refracture treatments are considered. Moreover, our results have shown that multiple refracture treatments can provide a viable means to improving the profitability of unconventional wells.

6. CONCLUSIONS

In this work, we have presented two optimization models for planning shale gas well refracture treatments. First, we proposed a novel forecast function for predicting pre- and post-refracturing productivity declines and a related continuous-time NLP model designed to determine whether or not a shale gas well should be refractured, and when exactly to perform the refracture treatment. We also presented a discrete-time, multiperiod MILP model that explicitly accounts for the possibility of multiple refracture treatments over the lifespan of a well. In the context of the latter, discrete-time model, we compared three alternative formulations: a big-M formulation as well as a disjunctive formulation transformed using Standard and Compact Hull-Reformulations. Applied to a representative well development project that considers the possibility of multiple refracture treatments, we found that the Compact Hull-Reformulation yields the best computational performance in terms of solution times.

The proposed modeling framework can be applied to planned, new well development projects, but also to existing, already producing wells to determine whether or not refracture treatments make economic sense. If, for instance, a price peak appears imminent in the near future, our modeling framework can help to decide whether the magnitude and extent of the projected price peak justifies a well restimulation. We applied the proposed MILP model to two case studies to demonstrate that refracturing can increase the expected ultimate recovery of a well over its lifespan by up to 25 %, and improve the profitability of a well development project by several hundred thousand USD. We find that the optimal number of refracture treatments and their timing are highly sensitive to the given natural gas price forecast. Therefore, our work is meant to lay the foundation for a more rigorous analysis of planning refracture treatments for field-wide development projects, considering price forecast uncertainty. At this time work is currently under progress to: (a) expand the proposed modeling framework in the context of stochastic programming to account for uncertain price forecasts and post-refracture well-performance, and (b) incorporate a reduced-order shale gas well and reservoir proxy model – such as those proposed by Knudsen and Foss[17] and Knudsen et al.[18] – directly into our model.

ACKNOWLEDGMENTS

Financial support from UNL, CONICET, the Scott Energy Institute at Carnegie Mellon University and the National Science Foundation under grant CBET-1437669 is gratefully appreciated.

NOMENCLATURE

Sets

$i \in I$	Refracture treatments
$t \in T$	Time periods

Binary variables

$x_{i,t}$	Active if well refractured for the *i*-th time in time period *t*
$y_{i,t}$	Active if in time period *t* the well has been refractured a total of *i* times
$z_{i,t,\hat{t}}$	Active if in time period *t* the well has been refractured a total of *i* times and the last refracturing occurred in time period $\hat{t}$

Continuous variables

P_t	Shale gas well production in time period *t*
trf	Timing of refracture treatment

Parameters

a	Production decline exponent
b	Post-refracturing decline change
d	Discount rate
k	Initial well production peak
r	Post-refracturing production peak
rt	Duration of refracture treatment
T	Expected lifespan of the shale gas well
$Q_{i,t,\hat{t}}$	Forecasted production of a well in time period *t* after a total of *i* refracture treatments when the last one occurred in time period $\hat{t}$
β	Post-refracturing peak reduction factor
γ	Initial fractures contribution

REFERENCES

1. Cafaro DC, Grossmann IE. Strategic planning, design, and development of the shale gas supply chain network. AIChE Journal. 2014; 60:2122-2142.
2. Drouven MG, Grossmann IE. Multi-Period Planning, Design and Strategic Models for Long-Term, Quality-Sensitive Shale Gas Development. AIChE Journal. 2016 (accepted for publication).
3. Jacobs T. Renewing Mature Shale Wells Through Refracturing. SPE News. 2014; May Issue.
4. Baihly J, Altman R, Malpani R, Luo F. Study assesses shale decline rates. American Oil & Gas Reporter. 2011; May Issue.
5. Dozier G, Elbel J, Fielder E, Hoover R, Lemp S, Reeves S, Siebrits E, Wisler D, Wolhart S. Refracturing works. Oilfield Review. 2003; 10(8):38-53.
6. Allison D, Parker M. Refracturing extends lives of unconventional reservoirs. American Oil & Gas Reporter. 2014; January Issue.
7. Sharma MM. Improved Reservoir Access Through Refracture Treatments in Tight Gas Sands and Gas Shales. Research Partnership to Secure Energy for America. 2013.
8. Eshkalak MO, Aybar U, Sepehrnoori K. An Economic Evaluation on the Re-fracturing Treatment of the U.S. Shale Gas Resources, SPE Eastern Regional Meeting. Society of Petroleum Engineers. 2014.
9. Tavassoli S, Yu W, Javadpour F, Sepehrnoori K. Well screen and optimal time of refracturing: a Barnett shale well. Journal of Petroleum Engineering. 2013; 2013:1-10.
10. Lantz T, Greene D, Eberhard M, Norrid S, Pershall R. Refracture treatments proving successful in horizontal Bakken wells. SPE Production & Operations. 2008; 23 (3):373-378.
11. Broderick J, Wood R, Gilbert P, Sharmina M, Anderson K, Footitt A, Glynn S, Nicholls F. Shale gas: an updated assessment of environmental an climate change impacts. A report commissioned by The Co-operative and undertaken by researchers at the Tyndall Centre, University of Manchester. 2011.
12. McCarl BA. Expanded GAMS User Guide Version 23.6. Washington, DC: GAMS Development Corporation, 2011.

13. WorldOil - Upstream News. Refracing fever sweeps across shale industry after oil collapse. http://www.worldoil.com/news/2015/7/07/refracing-fever-sweeps-across-shale-industry-after-oil-collapse (July 2015).
14. Raman R, Grossmann IE. Relation between MILP modelling and logical inference for chemical process synthesis. Computers & Chemical Engineering. 1991; 15 (2):73-84.
15. Grossmann IE, Trespalacios F. Systematic modeling of discrete-continuous optimization models through generalized disjunctive programming. AIChE Journal. 2013; 59 (9):3276-3295.
16. CME Group, Henry Hub Natural Gas Futures Quotes. 2016; available at: http://www.cmegroup.com/trading/energy/natural-gas/natural-gas.html [last accessed January 2016].
17. Knudsen BR, Foss B. Shut-in based production optimization of shale-gas systems. Computers & Chemical Engineering. 2013; 58:54-67.
18. Knudsen BR, Whitson CH, Foss B. Shale-gas scheduling for natural-gas supply in electric power production. Energy. 2014; 78:165-182.
19. Vecchietti A, Lee S, Grossmann IE. Modeling of discrete/continuous optimization problems: characterization and formulation of disjunctions and their relaxations. Computers & Chemical Engineering. 2003; 27:433-448.

APPENDIX: COMPACT HULL-REFORMULATION

In this section we study the Compact Hull Reformulation (CHR) in more detail, in an attempt to clarify: (a) when a CHR may generally be applied, and (b) what advantages and disadvantages it entails compared to alternative reformulations.

First, we assume that a given optimization problem involves a set of disjunctions $k \in K$ as shown in Eq. (40). Each of these disjunctions includes $j \in J_k$ disjunctive terms, all of which are linked by the logic OR-operator ($\vee$). Each disjunctive term is associated with a Boolean variable $Y_{jk} \in \{True, False\}$, which controls which disjunctive term is active, i.e., which constraints $A_{jk} x \leq b_{jk}$ are enforced. We note that Eq.

(40) is restricted to the linear case, i.e., all constraints $A_{jk}x \le b_{jk}$ involved in the disjunction are linear. Lastly, Eq. (41) ensures that no more than one disjunctive term $j \in J_k$ may be active for every disjunction $k \in K$.

$$\bigvee_{j \in J_k} \begin{bmatrix} Y_{jk} \\ A_{jk}x \le b_{jk} \end{bmatrix} \qquad \forall k \in K \tag{40}$$

$$\underline{\bigvee}_{j \in J_k} \qquad Y_{jk} \qquad \forall k \in K \tag{41}$$

The set of disjunctions in Eq. (40) may generally be transformed into mixed-integer constraints using a Big-M reformulation (BM), as shown in Eqs. (42)-(43), by introducing large parameters M_{jk}.

$$A_{jk}x \le b_{jk} + M_{jk}\left(1 - y_{jk}\right) \qquad \forall k \in K, j \in J_k \tag{42}$$

$$\sum_{j \in J_k} y_{jk} = 1 \qquad \forall k \in K \tag{43}$$

Alternatively, the set of disjunctions in Eq. (40) can be transformed using a Hull-Reformulation (HR), as displayed in Eqs. (44)-(46), by introducing a set of disaggregated variables v_{jk} for every disjunctive term.

$$x = \sum_{j \in J_k} v_{jk} \qquad \forall k \in K \tag{44}$$

$$A_{jk}v_{jk} \le b_{jk}y_{jk} \qquad \forall k \in K, j \in J_k \tag{45}$$

$$\sum_{j \in J_k} y_{jk} = 1 \qquad \forall k \in K \tag{46}$$

In general terms, the HR involves more variables and constraints than the BM, but its continuous relaxation is as least as tight as and generally tighter than the BM – as shown by Vecchietti, Lee and Grossmann[19]. For more details regarding Generalized Disjunctive Programming and a comparison of reformulations, we refer to the work by Grossmann and Trespalacios[15].

Given the set of disjunctions in Eq. (40) we argue that a Compact Hull-Reformulation (CHR) can only be applied if the coefficient matrix A_{jk} involved in the linear constraints $A_{jk}x \le b_{jk}$ is independent of the set of disjunctive terms $j \in J_k$, i.e., in this particular case $A_{jk} = A_k$. The CHR of the set of disjunctions in Eq. (40) is given by Eqs. (47)-(48).

$$A_k x \leq \sum_{j \in J_k} b_{jk} y_{jk} \qquad \forall k \in K \tag{47}$$

$$\sum_{j \in J_k} y_{jk} = 1 \qquad \forall k \in K \tag{48}$$

A noteworthy property of the CHR is that – compared to the standard Hull-Reformulation – it involves $|J_k| \times |K|$ fewer variables and $|J_k| \times |K|$ less constraints. However, it is important to note that the CHR is a "surrogate formulation", since the right-hand side of Eq. (47) is made up of aggregated constraints. Hence, it can be proven that the continuous relaxation of the standard HR is generally tighter than the continuous relaxation of the CHR. Yet, the significant reduction of the model size achieved by the CHR – both in terms of decision variables and model constraints – generally aids the performance of mixed-integer programming solvers such as CPLEX or Gurobi. Moreover, in direct comparison with the BM reformulation, we highlight the fact that the CHR does not require the specification of any big-M parameters.